Available online at www.sciencedirect.com
ScienceDirect
European Journal of Pharmaceutics and Biopharmaceutics 69 (2008) 1046–1056
European Journal of Pharmaceutics and Biopharmaceutics
www.elsevier.com/locate/ejpb

Research paper

Physicochemical characterization of five glyburide powders: A BCS based approach to predict oral absorption

Hai Wei [a], Chad Dalton [c], Marie Di Maso [c], Isadore Kanfer [d], Raimar Löbenberg [b,*]

[a] *Shanghai University of Traditional Chinese Medicine, Shanghai, China*
[b] *University of Alberta, Alta., Canada*
[c] *Merck Frosst, Canada, Pharmaceutical Research & Development, Que., Canada*
[d] *Rhodes University, South Africa*

Received 4 December 2007; accepted in revised form 22 January 2008
Available online 31 January 2008

Abstract

The purpose of this study was to investigate the suitability of physicochemical parameters of Active Pharmaceutical Ingredients (APIs) as input functions for the Advanced Compartmental Absorption and Transit Model (ACAT) to predict the oral absorption of drug products. Five different glyburide APIs were characterized using X-ray powder diffraction (XRPD), thermogravimetric analysis (TGA), differential scanning calorimetry (DSC), Raman spectroscopy, particle size and particle size distribution, specific surface area and true density measurements, as well as dissociation constant (pK_a), partition coefficient ($\log P$) and distribution coefficient ($\log D$). The computer simulations were performed using GastroPlus™. The results of XPRD, DSC and Raman spectroscopy indicated that no significant differences in crystal form were present in the five APIs. However, significant differences in particle size and particle size distribution were observed. A basic *in vitro*/*in vivo* relationship between the APIs' particle size and clinically observed plasma time profiles was established. The study demonstrates that *in silico* methods can assist the formulation scientist to set meaningful API specifications. Computer simulations could shorten the drug development process since appropriate bioawaivers, based on data from simulation studies, may be justified.

Keywords: Glyburide/glibenclamide; Oral absorption; Material characterization; Particle size; Advanced Compartmental Absorption and Transit model

1. Introduction

Glyburide (also known as glibenclamide) is a second-generation sulfonylurea. It is used orally as a hypoglycemic agent to treat non-insulin dependent (type II) diabetes mellitus [1,2]. Glyburide controls sugar levels by stimulating insulin secretion in the pancreas and increases tissue sensitivity to insulin [3]. Due to its low aqueous solubility [4] high bioavailability of up to 100% [2,4], and high permeability [5], glyburide can therefore be classified as a Class II drug based on the Biopharmaceutics Drug Classification System (BCS) [6].

As with class II drugs in general, glyburide's *in vivo* dissolution behavior could be the limiting/controlling factor for absorption and bioavailability [7]. Glyburide's solubility in gastrointestinal fluids and the pH in the gastrointestinal tract impact upon its *in vivo* dissolution [8]. Clinical studies using glyburide indicate a variability in bioavailability [9] and previous studies have demonstrated that the oral absorption of glyburide is formulation-dependent [10]. The dissolution behavior of different formulations has been correlated to oral performance and bioavailability of such products during a multinational postmarket comparative study [11]. Many scientific approaches have been applied for the enhancement of the solubility of glyburide

* Corresponding author. Faculty of Pharmacy and Pharmaceutical Sciences, University of Alberta, 3118 Dent/Pharm Building, Edmonton, Alta., Canada T6G 2N8. Tel.: +1 780 492 1255; fax: +1 780 492 1217.
E-mail address: rloebenberg@pharmacy.ualberta.ca (R. Löbenberg).

0939-6411/$ - see front matter © 2008 Elsevier B.V. All rights reserved.
doi:10.1016/j.ejpb.2008.01.026

to optimize *in vivo* dissolution and bioavailability [12]. These approaches include the addition of surfactants [13], complex formation with cyclodextrins [14], preparation of solid dispersion systems [15,16], micronisation [17], and crystalline-form conversion [18]. Processes such as spray-drying, milling and crystallization from different solvents have resulted in significant differences in the solid-state properties with regard to the solubility of glyburide [18,19]. The solubility of amorphous glyburide increases significantly compared to crystalline forms of the drug [20].

In vitro and *in vivo* correlations (IVIVCs) are highly desirable for the prediction of *in vivo* performance of a dosage form [5]. Such approaches can either be used in formulation development or retrospectively to reverse-engineer generic drugs. One way to predict the oral absorption of a drug involves the use of a mathematical model called Advanced Compartmental Absorption and Transit model (ACAT). It is commercially available under the name GastroPlus™.

The objective of this study was to investigate the solid-state properties of five pharmaceutical grades of glyburide. These five powders were either used or considered for use to produce commercial products by different manufacturers. As previously mentioned, the solid-state properties have significant influence on the bioavailability of glyburide products. In this manuscript we describe how an *in silico* method can be used to predict the oral performance of glyburide using powder properties and other *in vitro* data as input functions into the software. The simulations were compared with clinical data that were provided from manufacturers of some glyburide formulations.

2. Materials and methods

2.1. Materials

Five glyburide active pharmaceutical ingredients (APIs) were obtained from several sources: two from a German manufacturer (API-1: Lot 094; API-2: Lot 149, Hoechst AG, Frankfurt, Germany), two from South Africa (API-3: Lot IK1; API-4: Lot IK2, Comment: API-4 was milled from API-3) and API-5 (USP grade raw material: Lot RR302528/0, Fundação para o Remédio Popular (FURP), São Paulo State, Brazil).

Glyburide tablets were used as follows: Glyburide-1 (Euglucon N® 3.5 mg, Lot# 01N400, Boehringer Mannheim/Hoechs, Germany); Glyburide-2 (Glukovital® 3.5 mg, Lot#09601, Dr. August Wolff Arzneimittel, Bielefeld, Germany); Glyburide-3 (South African Test A 5.0 mg, Lot AA541; Dr. Isadore Kanfer, Faculty of Pharmacy, Rhodes University, South Africa); Glyburide-4 (South African Test B 5.0 mg, Lot AB341; Dr. Isadore Kanfer, Faculty of Pharmacy, Rhodes University, South Africa).

Sodium taurocholate (crude) was purchased from Sigma–Aldrich (St. Louis, Missouri, USA). Egg-lecithin 60% was purchased from ICN (Aurora, Ohio, USA). Potassium dihydrogen phosphate, potassium chloride, sodium chloride, sodium hydroxide, phosphoric acid and hydrochloride acid (analytical grade) were purchased from BDH (BDH Inc. Toronto, Canada).

2.2. Scanning electron microscopy (SEM)

Samples were evaluated using a JEOL JSM5900-LV scanning electron microscope (SEM, JEOL LTD., Tokyo, Japan). Analysis was carried out in low vacuum mode at 20 Pa using a voltage of 15 kV. The APIs were uniformly spread on the surface of insulated double-sided carbon tape. No sputter coating was required. Micrographs were acquired at 500× magnification.

2.3. X-Ray powder diffraction (XRPD)

XRPD patterns were measured using a Scintag XDS-2000 spectrometer (Thermo ARL, Ecublens, Switzerland). The instrumental conditions were as follows: Si (Li) Peltier – cooled solid-state detector; CuK_{α} source at a generator power of 45 kV and 40 mA; divergent beam (2 and 4 mm) and receiving beam slits (0.5 and 0.2 mm); scan range set from 2 to 40° 2θ with a step size of 0.02° and a count time of 2 s. The APIs were uniformly dispersed on a quartz disk.

2.4. Thermogravimetric analysis (TGA)

A Perkin Elmer Diamond Thermogravimetric/Differential Thermal Analyzer (TG/DTA, Perkin Elmer Instruments, Wellesley, Massachusetts, USA) using a heating rate of 10 °C/min from 30 to 315 °C under nitrogen at 100 mL/min was used. The instrument balance was verified using a 20 mg standard weight and indium and tin were used for temperature calibration.

2.5. Differential scanning calorimetry (DSC)

The thermal behavior was investigated using a TA robotic differential scanning calorimeter (Q 1000, TA Instrument Inc., New Castle, Delaware, USA). DSC analyses (sample: 5 mg, $n = 2$) were carried out in aluminium pans under nitrogen at a flow rate of 50 mL/min. The temperature and heat flow were calibrated with indium and tin. The samples were analyzed from 30 to 185 °C using a heating rate of 10 °C/min. The amorphous form of glyburide was prepared by DSC following the modified melting and quench cooling method [8,12]. Samples (5 mg) were heated in aluminium pans at 10 °C/min to 185 °C (complete melt) and then cooled to room temperature at 10 °C/min.

The glass transition of the amorphous form was measured by reheating the amorphous melt using three heating rates (20, 50 and 100 °C/min) as shown in Fig. 4. The furnace temperature was cooled to 30 °C between each successive heating cycle past the compound's glass transition temperature. A similar method was applied to all glyburide

lots to ensure the absence of amorphous content which could drastically affect the dissolution of the API.

2.6. Raman spectroscopy

A Bruker RFS 100/S FT-Raman spectrometer (Bruker Optics Inc., Billerica, Massachusetts, USA) was used along with BrukerQuant 2 software for spectral analysis. The laser power was set to 250 mW with a scan range from 3500 to 0 cm^{-1}, a scan resolution of 4 cm^{-1}, an aperture setting of 3.5 and a scan number of 64–256. Raman spectra for both the surface of intact and ground glyburide tablets were recorded by averaging three measurements. The surface of the tablets was analyzed by spectrally averaging three different positions on the tablet's surface, the powders were re-packed and re-analyzed 3 times in 2-mm diameter metal sample holders to ensure reproducibility of the results and minimize the effects of sample inhomogeneity. Spectral processing using first derivative and vector normalization was applied to the spectra prior to analysis.

2.7. Particle size analysis

The particle size and particle distribution of the glyburide APIs were analyzed by a particle size analyzer (COULTER® LS 230 Particle Size Analyzer, Coulter Corporation, Fullerton, California, USA).

Suspensions of the glyburide APIs were prepared in a solvent (0.1% w/v) solution consisting of lecithin in 2,2,4-trimethylpentane. The particles were well-dispersed and no significant agglomerates were present in the solution. Continuous agitation at 50 rpm was applied during measurements and the particle size distribution data were presented as means, 10% (D10), 25% (D25), 50% (D50), 75% (D75) and 90% (D90) of the particle volume undersize. The percentage volume undersize is the percentage of the total volume of particles in the distribution profile below a specific particle size.

2.8. Specific surface area measurement

Measurement of the specific surface area of solids was performed with a Quantachrome Autosorb-1 surface area and pore size analyzer (Quantachrome Instruments, Boynton Beach, Florida, USA). The instrument was connected via the lower back panel to nitrogen and helium lines (both regulated at 10 PSI). The vacuum gauges were set to 10 and 100 millitorr, respectively. The cold trap, which was filled with liquid nitrogen during operation, was maintained at 77 K to trap impurities from the gas lines. The instrument was calibrated using standard powders obtained from Quantachrome for multipoint BET (Brunauer, Emmett and Teller equation) analysis. The surface area of the standard reference was 2.17 m^2/g with a 95% reproducibility limit of 0.19 m^2/g (Quantachrome catalogue No. 20007: lot No. 3101, Quantachrome Instruments, Boynton Beach, Florida, USA).

2.9. True density measurement

The true densities of the glyburide APIs were measured with a Quantachrome Ultrapycnometer 1000 (Quantachrome Instruments, Boynton Beach, Florida, USA) under helium at 18 psi and the samples were stored in desiccators overnight. Duplicate measurements were performed at 23.7 °C using a flow purge of 30 min.

2.10. Dissociation constant (pK_a), partition coefficient ($\log P$) and distribution coefficient ($\log D$)

The pK_a, $\log P$ and $\log D$ of glyburide APIs were measured by spectrophotometric titrations using a Sirius flagship instrument for pK_a and $\log P$ measurement using pH-metric technology (GLpK_a) in combination with a D-Pas detector (Sirius Analytical Instruments Ltd., East Sussex, UK). Data acquisition was achieved with Refinement Pro software V1.104 (Sirius Analytical Instruments Ltd., East Sussex, UK). UV absorbance measurements were performed using a fiber optic probe and photodiode array detector (Sirius Analytical Instruments Ltd, East Sussex, UK) equipped with a deuterium lamp. Titrations using different concentrations of KOH or HCl were performed in aqueous media consisting 0.15 M KCl under argon 60 mL/min, at 25 °C.

2.11. Solubility determination

Twenty milligrams (excess) API-2 was added to 10 mL of FaSSIF (fasted state simulated intestinal fluid containing 3 mM sodium taurocholate and 0.75 mM lethicin [7] at pH 1.7, 5.0, 6.5, 7.4 and stirred overnight (12 h) at 37 ± 0.5 °C in a water bath. The pH of each sample was checked during the experiment and the resulting solution was then filtered through a 0.22 μm Millex-GP membrane filter (Millipore, Bedford, MA, USA). The filter membrane was checked for glyburide adsorption (known concentrations of the samples were checked by HPLC before and after filtration) and solubility was determined by HPLC analysis.

2.12. Computer simulations

The *in vitro* data were applied to previously used simulation protocols [21] accordingly adapted. GastroPlus™ (version 5.1, Simulations Plus Inc., Lancaster, California, USA) was used to estimate absorption and pharmacokinetics of the five APIs. The program requires insertion of the relevant physicochemical, physiological and pharmacokinetic input data in specific spread sheets provided in the software program. These data include properties such as the physical and chemical characteristics of the APIs, gastrointestinal permeability and the relevant dose information. Bulk density, solubility, pK_a, $\log D$, particle size and particle distribution were obtained from the material characterization described above. The human permeability

(P_{eff}) of glyburide was estimated as 3.5×10^{-4} cm/s [21]. The solubility-pH profiles of glyburide were obtained as previously described [21] and the diffusion coefficient of glyburide was estimated using GastroPlus™ The same dose as administered in the clinical studies was used for the simulations.

The immediate release dosage form model was selected in GastroPlus™. The physicochemical data including pK_a, log D, solubility, particle size distribution and the drug dose were used by the software to calculate the drug concentration in each compartment. Pharmacokinetic data were obtained from clinical studies performed on products containing the relevant glyburide APIs [11,22]. Glyburide-1 and 2 products (dose 3.5 mg) containing API-2 and glyburide-3 and 4 products (dose 5 mg) from South Africa containing API-3 and API-4. Pharmacokinetic parameters of the clinically observed data such as volume of distribution, clearance and micro-constants (Table 1) were obtained by fitting the observed clinical data to a two-compartmental pharmacokinetic model using the Kinetica software package (version 4.4.1, InnaPharse Corporation, Philadelphia, Penesylvania, USA). The obtained data were entered into the pharmacokinetic spreadsheet in GastroPlus™.

Since the simulation study uses data from different *in vivo* studies where different dosage forms were tested in different volunteers it is justified that the individually fitted data were used in the simulations rather than one generic set of parameters for all simulations.

In the "Physiological Data" input spreadsheet, the human fasted state model was chosen and the default values for transit time and pH were selected for each compartment. The recommended absorption scale factor model, (log D model) was chosen to account for absorption.

2.13. Statistics

Percent Prediction Error (%PE) was calculated according to the FDA Guidance for industry using Eq. (1) [23]

$$\mathrm{PE} = \frac{\text{Observed} - \text{Predicted}}{\text{Observed}} \times 100\% \quad (1)$$

Linear regression analysis for the observed vs. simulated data using a 95% confident interval was performed using Excel (Microsoft Inc. Seattle, Washington, USA).

In all cases, significance of difference between experiments was calculated by Student's t test using two-tailed distributions and two-sample equal variance (Microsoft Excel, Version 2000, Microsoft Inc. Microsoft Inc. Seattle, Washington, USA). Statistical significance was calculated at the 95% ($p < 0.05$) confidence level.

3. Results

3.1. Surface area, true density, particle size

The SEM micrographs were used to determine the particle size and morphology of the five glyburide APIs (Fig. 1). All five APIs consisted of irregularly shaped particles. However, each glyburide API had different particle sizes and size distributions which might be due to the different manufacturing or milling processes [24]. API-1 had the largest particle size and widest particle size distribution (Table 2). API-1 was the least cohesive powder due to its larger particle size. The particle size and size distributions of API-2 and API-5 were similar, but more of the larger particles existed in API-5 samples. The particle size and size distributions of API-3 and API-4 were smaller compared to the other three APIs. API-4 had more smaller and uniform particles compared to API-3. This was confirmed by the processing information obtained from the supplier who stated that API-4 was made by milling API-3.

The physicochemical parameters of the five glyburide APIs including specific surface area, true density and particle size and particle size distribution are given in Table 2. API-1 contained the biggest particles and had the widest size distribution followed by API-5, API-2, API-3 and API-4. The surface area of API-1 was the smallest followed by API-5, API-2, API-3 and API-4 which confirms the visual observation using SEM data. Particle size, surface area and SEM data confirmed that API-4 was produced by milling API-3.

3.2. Crystallinity and form determination

XRPD was used to determine the extent of crystallinity and the identity of crystalline forms present in the five APIs (Fig. 2) [12]. The XRPD results showed no distinguishable differences in the diffraction patterns between the different APIs. There were no detectable amounts of amorphous drug in the API samples. This indicated that all five APIs consisted of the same crystalline form. However, XRPD might not be sensitive enough to detect small quantities of different crystal forms or small amounts of amorphous drugs. Typically the detection limit of this method for the

Table 1
Pharmacokinetic parameters of different products used for the computer simulations

	C_{max} (ng/mL)	AUC_{0-n} (ng/mL h)	Clearance (L/h)	V_c (L)	K_{12} (h^{-1})	K_{21} (h^{-1})
Glyburide-1 (API-2)	301	1359.6	2.17	4.68	0.379	0.103
Glyburide-2 (API-2)	221	1441.3	1.64	6.18	0.161	0.069
Glyburide-3 (API-3)	95	563.8	7.40	2.31	0.406	0.235
Glyburide-4 (API-4)	196	1067.0	3.91	9.69	0.151	0.043

The mean values of the clinical data obtained from these four products were well described by a two-compartmental model [32].

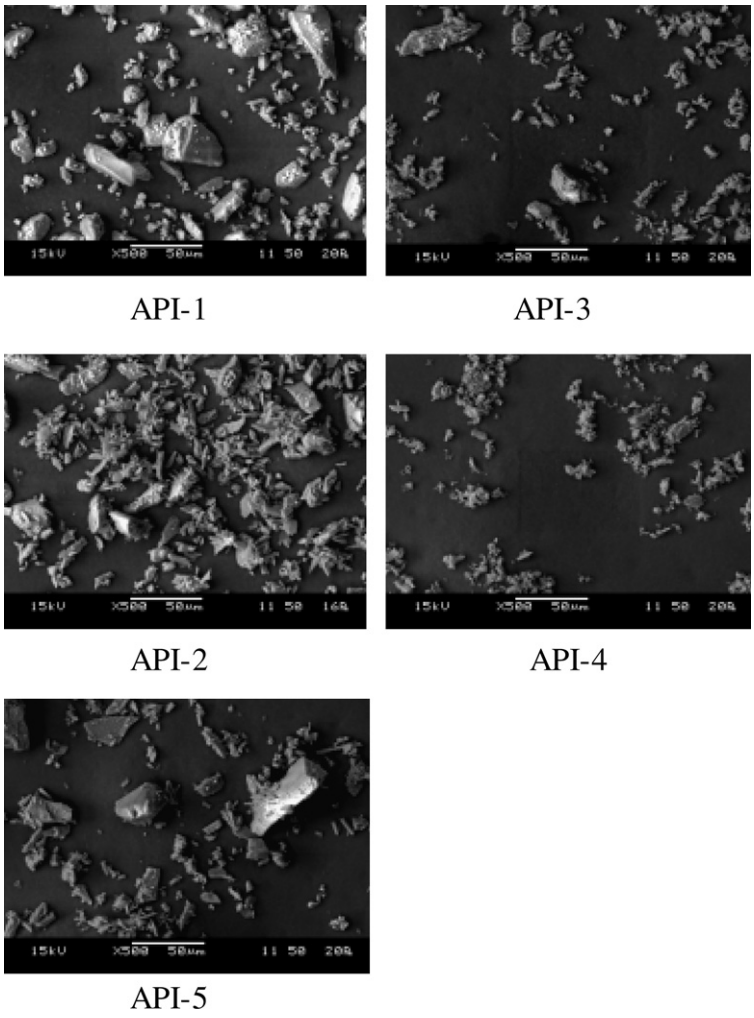

Fig. 1. Particle size and appearance of the five glyburide powders using SEM.

Table 2
Physicochemical data determined for five glyburide APIs

	True density ($n = 2$, g/mL)	Surface area (m^2/g)	Mean particle size and SD (μM)	D10 (μM)	D25 (μM)	D50 (μM)	D75 (μM)	D90 (μM)
API-1	1.35	0.45	22.65 ± 25.39	0.96	2.82	11.73	36.66	61.77
API-2	1.38	1.67	12.55 ± 12.87	1.31	3.47	8.41	17.47	29.69
API-3	1.35	3.48	5.18 ± 5.19	0.88	1.84	3.63	6.61	11.35
API-4	1.35	3.96	4.25 ± 3.97	0.76	1.49	2.94	5.57	9.75
API-5	1.36	1.53	15.10 ± 16.80	1.15	3.20	8.71	20.95	39.12

detection of amorphous forms requires at least 10% amorphous content [25].

Raman spectroscopy can be used to investigate both chemical and physical characteristics of solid-state materials. Szép et al. reported that the characteristic bands of commonly used excipients such as lactose monohydrate and corn starch are below 1500 cm^{-1} [26]. In order to avoid any overlap with excipients, the measured range, 1650–1500 cm^{-1}, a range associated primarily with carbon-carbon double bonds and phenyl ring stretching and breathing, was selected. The acquired whole Raman spectra of the five APIs were almost identical (Fig. 3) and the spectra for the API in the tablets were almost identical to the API raw material spectra. However, all the above spectra were remarkably different from the spectra of the amorphous forms produced, where a shift to the high wave number was observed (Fig. 4). These results indicated that all the APIs were constitutionally similar which is in agreement with the results from XPRD.

3.3. Thermal analysis

Considering instrument variability, the acquired TGA spectra (data not shown) from all five APIs were similar.

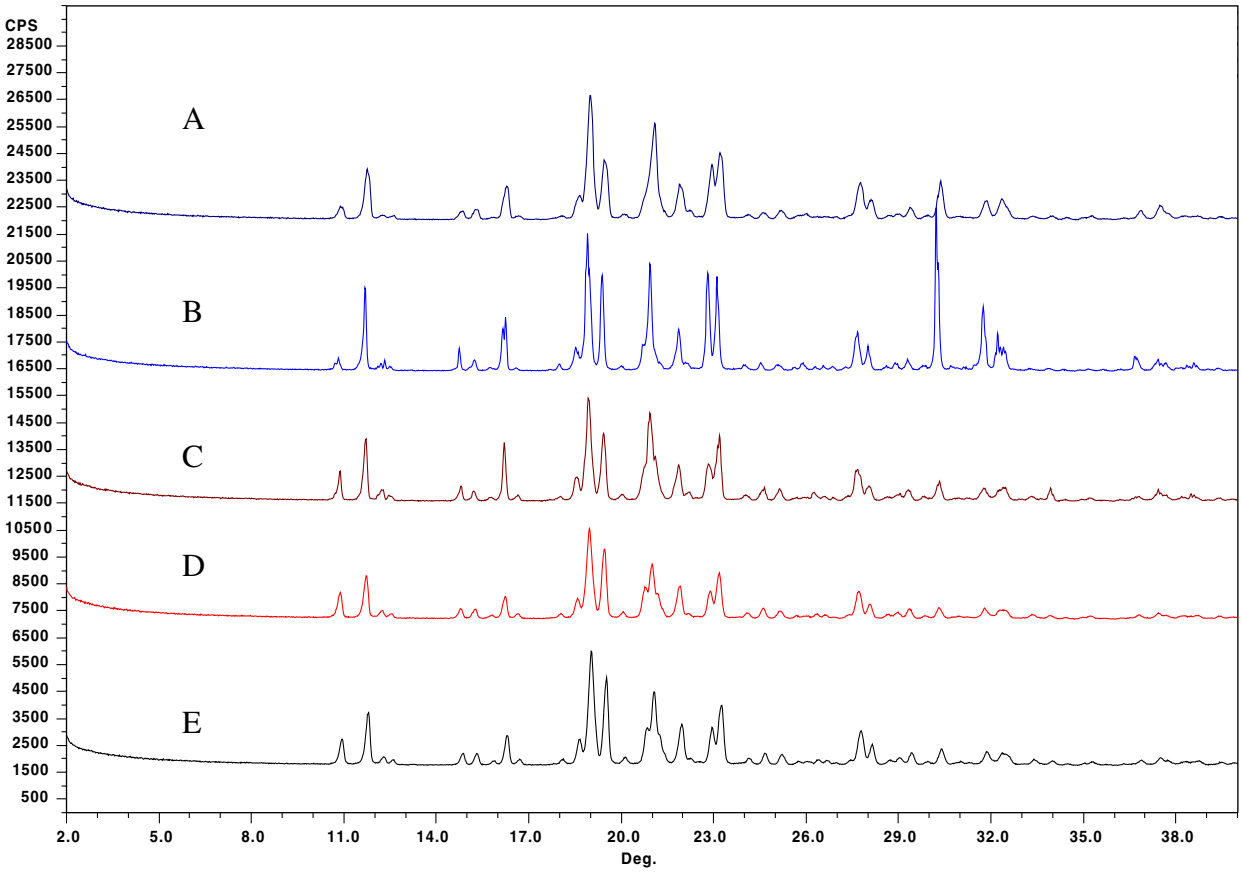

Fig. 2. Comparison of X-ray diffraction spectra of five glyburide APIs (A:API-2; B:API-1; C:API-5; D:API-4; E:API-3).

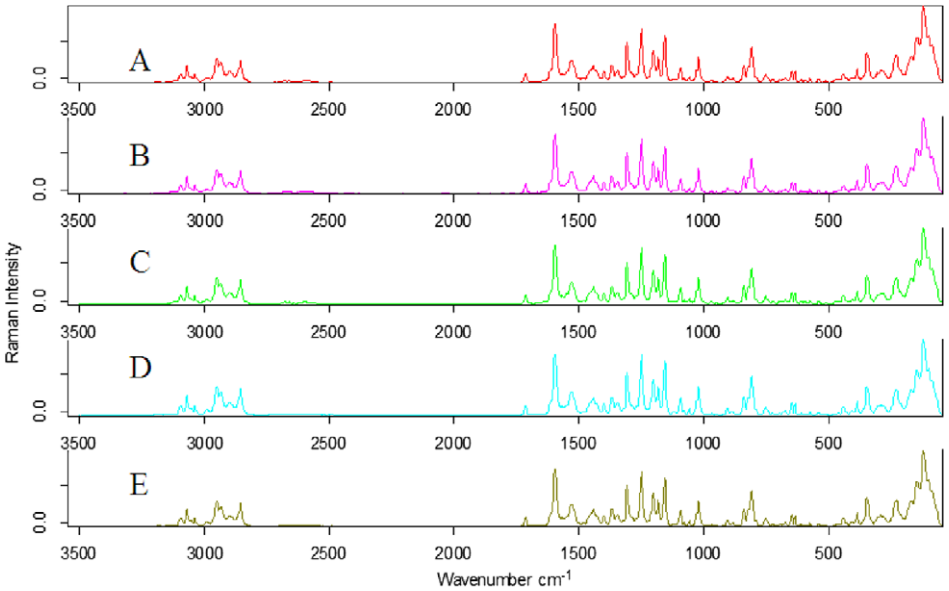

Fig. 3. Comparison of the Raman spectra for five glyburide APIs (A:API-3; B:API-4; C:API-5; D:API-1; E:API-2).

One common thermal property of all five APIs was that they degraded above the melting point (175 °C). The onset of the degradation temperature range was from 195 to 200 °C. The weight loss from 30 °C to melting point (175 °C) was negligible and probably due to the low volatile content and non-hygroscopic nature of glyburide.

The entire range (30–185 °C) of the DSC curves (data not shown) for all five APIs showed only one single sharp endothermic peak at 175 °C, corresponding to its melting

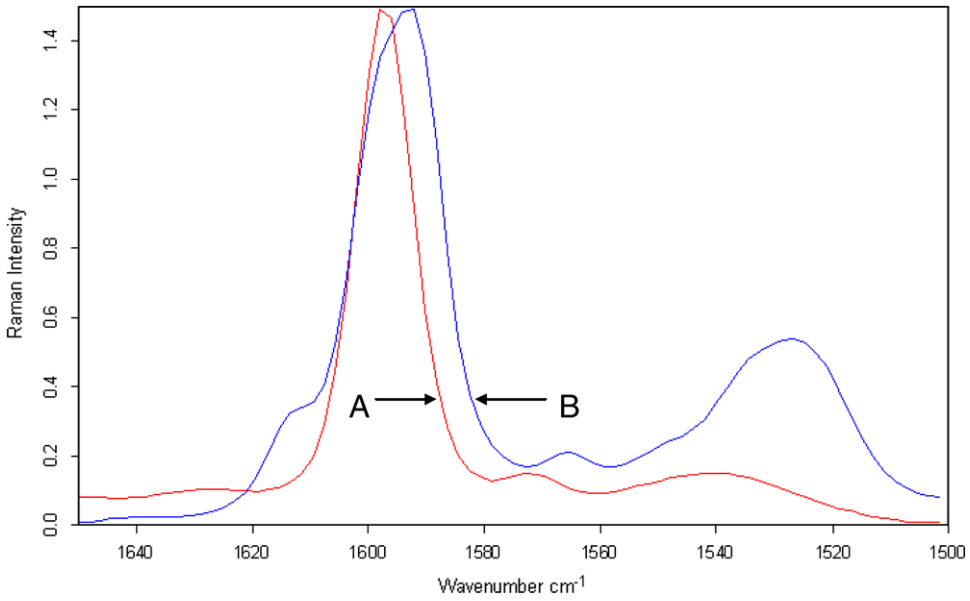

Fig. 4. Comparison of the Raman spectra for glyburide amorphous form and API-1 (A:glyburide amorphous form; B:API-1).

point. There were no glass transition (Tg) or recrystallisation exothermic peaks in the DSC curves which confirmed that no amorphous forms were present in the APIs [24]. The DSC curves (range from 160 to 185 °C) of the APIs are shown in Fig. 5. The enthalpy (ΔH) of all five APIs was determined as: API-1 (90 J/g), API-2 (99 J/g), API-3 (98 J/g), API-4 (102 J/g), and API-5 (92 J/g). Although API-1 had the lowest enthalpy, no amorphous content was detected by any of these methods described in this manuscript. The lower enthalpy may simply be due to greater crystalline defects relative to the other glyburide batches. The endothermic peak of the crystalline API corresponding to its melting point will broaden with the reduction of enthalpy if the amorphous drug or other impurities are present [15]. The endothermic peak of API-4 was the sharpest. The endothermic peaks of API-1 and API-5 were broader compared to the others but the difference can be considered minor. The amorphous form of glyburide API was produced by a modified Melting and Quench Cooling method [8,12]. Detection of the amorphous form can be achieved by applying high ramp temperature rates to the samples [27]. In this study, ramp rates (20, 50 and 100 °C/min) were applied for each heating and cooling cycle. The glass transition temperature of the amorphous form obtained from the Melting and Quench Cooling method using this cycle temperature program was determined to be about 60 °C. The glass transition curve of the amorphous form was sharper when the ramp rate increased, especially at 100 °C/min (Fig. 6). The same temperature program was applied to the five APIs. No glass transition curves were detected even at the highest ramp rate. This indicates that the APIs do not contain any detectable or appreciable amounts of amorphous material.

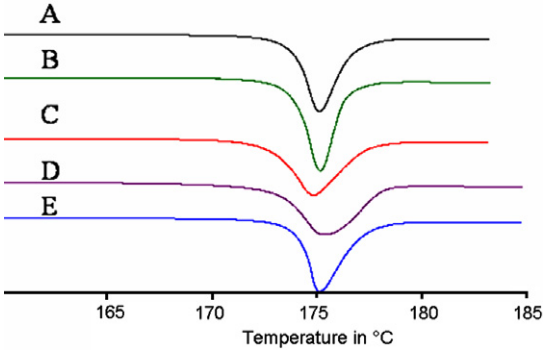

Fig. 5. Comparison of five glyburide APIs using DSC (A:API-3; B:API-4; C:API-5; D:API-1; E:API-2).

3.4. pK_a, log P and log D measurements

The pK_a and $\log P$ of the glyburide APIs were 5.1 and 4.5, respectively. This is in agreement with data reported in the literature (pK_a 5.3) [4]. The $\log D$ profile was derived from the pK_a and $\log P$ data (data not shown).

3.5. Computer simulations

The predicted plasma time curves were compared with the *in vivo* data obtained from drug concentrations in plasma data following administration of the relevant products to healthy volunteers [11,22]. Fig. 7 shows the observed and predicted data for API-2. The API-2 from this manufacturer was used in the glyburide-1 product of an *in vivo* bioequivalence study. The simulation of the glyburide-1 product predicts C_{max}, T_{max} and AUC_{0-24} within prediction errors of 1.9%, 20% and 9.4%, respectively. Raman spectroscopy was used to compare the drug powders in glyburide 1 and 2 products (data not shown). The results suggest that the API in both products were similar.

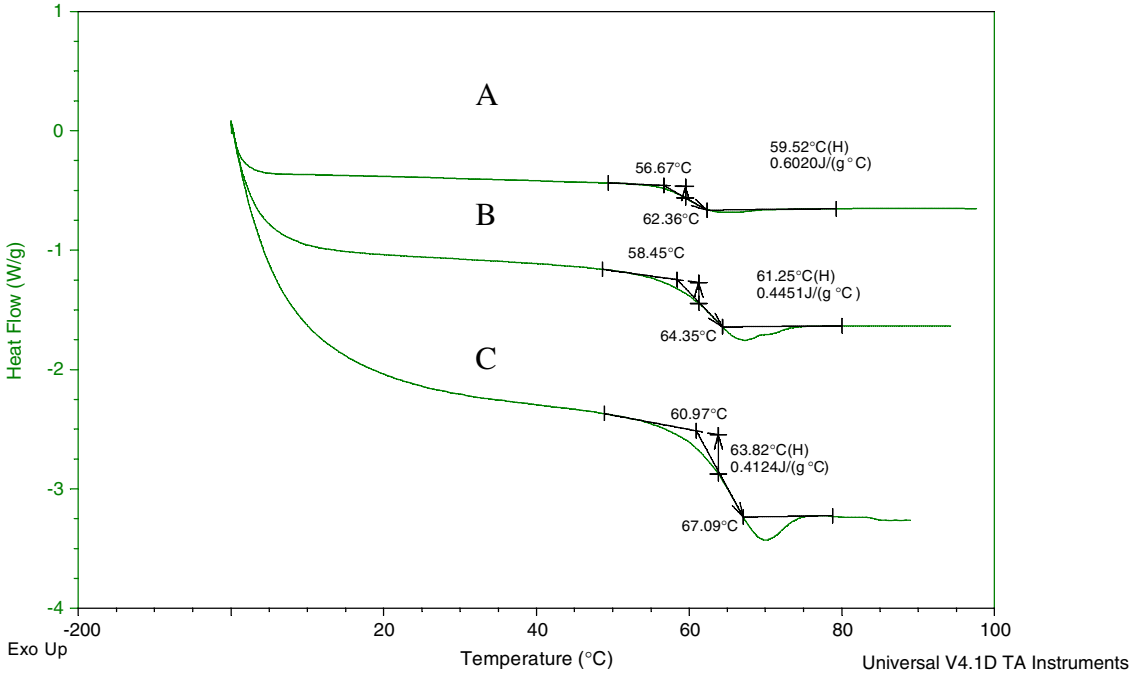

Fig. 6. Glass transition curves of amorphous glyburide obtained at different heating rates (A:20 °C/min; B:50 °C/min; C:100 °C/min).

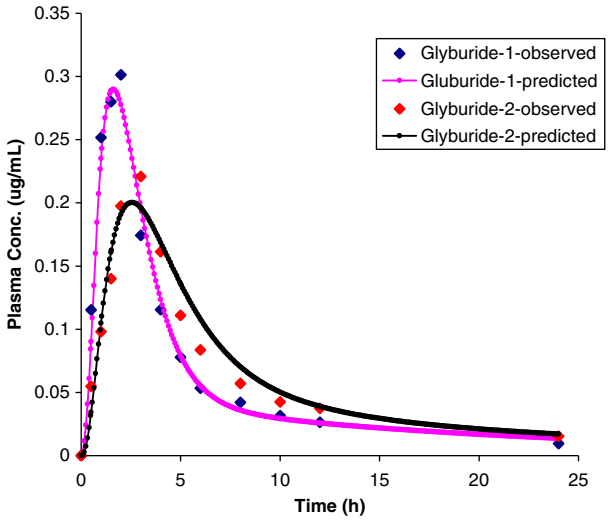

Fig. 7. Comparison of the simulated and observed data for glyburide-1 and 2 products containing API-2 using physicochemical data as input for the simulation.

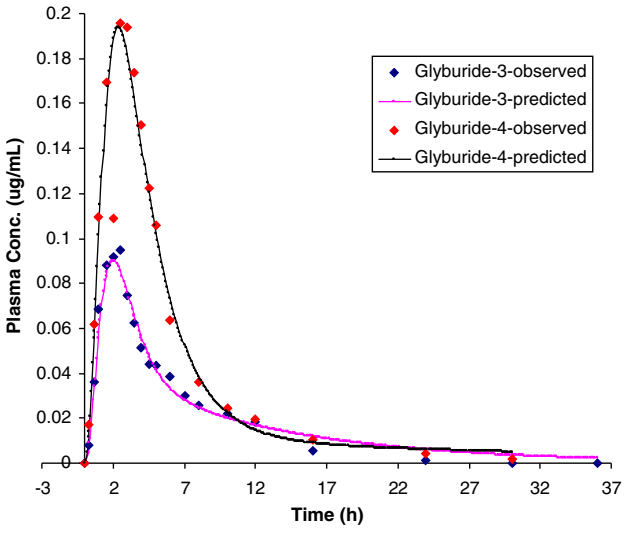

Fig. 8. Comparison of the simulated and observed data for glyburide-3 and 4 products containing API-3 and API-4 using physicochemical data as input for the simulation.

Based on this assumption the oral performance of the glyburide-2 product was simulated using its clinically observed PK data and the physicochemical input data of API-2. As shown, the simulation predicts C_{max}, T_{max} and AUC_{0-24} within prediction errors of 9.4%, 15% and 6.4%, respectively. The differences between both products seem to be formulation dependent e.g. use of different excipients which might cause different pharmacokinetic profiles. Fig. 8 shows simulations of the glyburide-3 and glyburide-4 containing API-3 and API-4, respectively. As mentioned previously, API-4 was milled from API-3. API-4 had a smaller particle size and particle size distribution. Bioavailability studies on these two products were performed in a different set of subjects. This might explain the differences in the observed profiles. However, the absorption patterns calculated by the ACAT model were found to be similar for both products. Absorption patterns are defined as the fraction dose absorbed in each segment of the *in silico* gut and the patterns are mainly influenced by solubility and particle size. The simulations for API-3 and API-4 predict C_{max}, T_{max} and AUC within prediction errors of 4.6% and 0.8%, 20% and 4.0%, 15.2% and 2.3%, respectively. The

simulation results using only the *in vitro* data as input functions showed that the *in silico* model was suitable to predict the oral absorption of four glyburide products.

4. Discussion

Glyburide is absorbed throughout the entire gastrointestinal tract [28] therefore; it is a good model drug for simulation using the ACAT model. The literature describes different crystal and amorphous forms of glyburide. Chikhalia et al. discussed that the milling processes could activate the surface of drug particles by energy transfer and form a peripheral disordered layer that had amorphous characteristics [24]. APIs containing amorphous forms and peripheral disordered layers might have greater weight loss than pure crystals when the temperature increased. Such effects can be detected by sublimation of the amorphous layer and will change the TGA thermogram. API-4 which was milled from API-3 showed the same thermal property in the TGA analysis compared to API-3. The results of XPRD, DSC and Raman spectroscopy indicated that no differences in the composition existed between the five investigated APIs. The possibility of polymorphism can be eliminated based on the material characterizations. Panagopoulu-Kaplani et al. [12] reported crystal form conversions during the production and storage of glyburide in tablets. The solubility of such recrystallized API had changed significantly. The results obtained in the present study derived from Raman spectra showed there were no significant crystal conversions during the production and storage of the products investigated.

The material characterizations using SEM, particle size and size distribution analysis further showed that significant differences between the APIs were detected only for the particle size and particle size distribution. A reduced particle size of an API can improve the solubility and intrinsic dissolution rate; therefore an influence on the drug's bioavailability may be expected [29]. Pharmaceutical preparations which used micronized glyburide showed better absorption, less variability and required a lower dose compared to non-micronized glyburide [30]. Timmins et al. showed that controlled particle size distribution can significantly influence the reproducibility of a product's bioavailability [20]. Balan et al. optimized glyburide formulations as shown by comparing the bioavailability of different formulations that contained different particle sizes of glyburide [31]. They showed that a controlled particle size and size distribution reduced the variability in bioavailability. Table 3 shows an example of the possible impact on drug absorption when the particle size or particle size distribution of the product containing API-3 changed. In the first case the particle size theoretically decreased (down to 25%) or increased (up to 400%) while size distribution was kept constant, in the second case the particle size distribution theoretically decreased (down to 25%) or increased (up to 400%) while the mean particle size was kept constant. The theoretically predicted impact on C_{max}, AUC and T_{max} is shown in Table 3. The influence of the particle size and size distributions on the AUC and C_{max} is similar. Particle size has, as expected, a more pronounced influence on T_{max} compared to an increase in particle size distribution. Such simulations may be used by formulation scientists to set particle size and particle size distribution specifications for APIs and allow predictions to be made when an API's particle size or particle size distribution may cause an unacceptable deviation from the observed plasma concentrations vs. time. In early drug development such simulations can be used to estimate plasma concentration levels and can help to define which formulation approach could be used to develop a suitable drug product. This can shorten the time needed for the drug development process because biowaivers may be justified on the basis of simulation studies [20,31]. Another application of such simulations might be the optimization of an existing dosage form or the pre-selection of a dosage form for a drug under development. Here the formulation scientist can use the pre-defined dosage form models of the software to improve drug plasma concentration vs. time curves. Examples are gastric drug release from a floating dosage form or simulation of the passage through the gastrointestinal tract of a dispersed vs. an integral dosage form. However, it has to be pointed out that such simulations have to assume that the dosage form does not impact the pharmacokinetic parameters. The last example for the application of predic-

Table 3
Simulated impact of changes in particle radius and particle size distribution ± standard deviation (SD) on the oral performance of a glyburide product containing API-3

Particle Radius (μM) ± SD	0.65 ± 2.6	1.3 ± 2.6	2.6 ± 2.6 (mean)	5.2 ± 2.6	10.4 ± 2.6
AUC_{0-36}	650.1 (+0.1%)	649.9 (+0%)	649.2	646.2 (−0.5%)	622.5 (−4.1%)
C_{max}	97 (+7.8%)	95 (+5.6%)	90	79 (−12.2%)	57 (−36.7%)
T_{max}	1.8 (−10%)	1.9 (−5.0%)	2.0	2.4 (+20%)	3.5 (+75%)
Mean particle radius (μM) ± SD	2.6 ± 0.65	2.6 ± 1.3	2.6 ± 2.6 (mean)	2.6 ± 5.2	2.6 ± 10.4
AUC_{0-36}	650.2 (+0.2%)	650.1 (+0.1%)	649.2	643.4 (−0.9%)	612.9 (−5.6%)
C_{max}	101 (+12.2%)	98 (+8.9%)	90	77 (−14.4%)	61 (−32.2%)
T_{max}	1.9 (−5%)	1.9 (−5%)	2.0	2.16 (+8%)	2.4 (+20%)

The measured particle size "mean" and the particle size distribution were theoretically manipulated. The simulated values are listed and the % change compared to the mean value are given in brackets. C_{max} (ng/mL); AUC_{0-n} (ng/mL h); T_{max} (h).

tive simulations is reverse engineering of drug products. If the physicochemical data for API-1 were used in the simulations (data not shown) the resulting plasma concentration vs. time curve would be significantly different from the other APIs. Products made with API-1 probably do not meet current bioequivalence criteria to manufacture glyburide-1 or glyburide-2 products. However, based on the simulations it can be assumed that if API-5 will be used in these two products they will be bioequivalent (data not shown). This assumption is based on the very similar physicochemical properties of API-2 and API-5. However, currently no clinical data are available to prove this for API-1 and API-5. Formulation scientist can input the physicochemical data of the API they intend to use and predetermine if it has an appropriate particle size and size distribution. This can assist in defining further manufacturing processes such as the necessity of milling.

5. Conclusion

The material characterizations of five glyburide APIs showed the absence of crystalline differences between the APIs studied. However, the five APIs showed differences in surface area, particle size and size distributions. Such differences might influence the dissolution and bioavailability of glyburide. Particle size, being a key parameter for drug dissolution, was used in the ACAT model to predict the oral performance of different glyburide products. A basic *in vitro*/*in vivo* relationship between the API particle size and clinically observed plasma versus time profiles was established for three APIs. The information obtained by such *in silico* models can be valuable for formulation scientists to set meaningful API specifications, develop optimized drug products or to reverse engineer generic versions of existing products.

Acknowledgements

The authors like to thank Simulation Plus Inc. (USA) for making their software available and Cynthia Bazin, Rafik Naccache and Karine Khougaz, members of the PR&D group at Merck Frosst, Canada for their help and their valuable comments on the material characterizations. The study was partially sponsored by a collaborative grant between NSERC and Merck Frosst.

References

[1] J.G. Pearson, Pharmacokinetics of glyburide, Am. J. Med. 79 (Suppl. 3B) (1985) 67–71.
[2] P.J. Neuvonen, K.T. Kivisto, The effects of magnesium hydroxide on the absorption and efficacy of two glibenclamide preparations, Br. J. Clin. Pharmacol. 32 (1991) 215–220.
[3] S.N. Davis, D.K. Granner, Insulin, oral hypoglycemic agents and the pharmacology of endocrine pancreas, in: A.G. Gilman (Ed.), The Pharmacological Basis of Therapeutics, ninth ed., McGraw-Hill, New York, 1996, pp. 1487–1518.
[4] .R. Löbenberg, J. Krämer, V.P. Shah, G.L. Amidon, J.B. Dressman, Dissolution testing as prognostic tool for oral drug absorption: dissolution behavior of glibenclamide, Pharm. Res. 17 (4) (2000) 439–444.
[5] H. Vogelpoel, J. Welink, G.L. Amidon, H.E. Junginger, K.K. Midha, H. Möller, M. Olling, V.P. Shah, D.M. Barends, Biowaiver monographs for immediate release solid oral dosage forms based on biopharmaceutics classification system (BCS) literature data: verapamil hydrochloride, propranolol hydrochloride and atenolol (Commentary), J. Pharm. Sci. 93 (8) (2004) 1945–1956.
[6] R. Löbenberg, G.L. Amidon, Modern bioavailability, bioequivalence and biopharmaceutics classification system. New scientific approaches to international regulatory standards, Eur. J. Pharm. Biopharm. 50 (2000) 3–12.
[7] E. Galia, E. Nicolaides, D. Hörter, R. Löbenberg, C. Reppas, J.B. Dressman, Evaluation of various dissolution media for predicting *in vivo* performance of class I and II drugs, Pharm. Res. 15 (5) (1998) 698–705.
[8] J.E. Patterson, M.B. James, A.H. Forster, R.W. Lancaster, J.M. Butler, T. Rades, The influence of thermal and mechanical preparative techniques on the amorphous state of four poorly soluble compounds, J. Pharm. Sci. 94 (9) (2005) 1998–2012.
[9] Drug Information for Health Care Professional, USP DI, vol. I, 1999.
[10] G. Neugebauer, G. Betzien, V. Hrstka, B. Kaufmann, E. Von Möllendorff, U. Abshagen, Absolute bioavailability and bioequivalence of glibenclimide (Semi-Euglucon®N), Int. J. Clin. Pharmacol. Ther. Toxicol. 23 (9) (1985) 453–460.
[11] H. Blume, S.L. Ali, M. Siewert, Pharmaceutical quality of glibenclamide products: a multinational postmarket comparative study, Drug. Dev. Ind. Pharm. 19 (1993) 2713–2741.
[12] A. Panagopoulou-Kaplani, S. Malamataris, Preparation and characterization of a new insoluble polymorphic form of glibenclamide, Int. J. Pharm. 195 (2000) 239–246.
[13] J. Singh, Effect of sodium lauryl sulfate and Tween® 80 on the therapeutic efficacy of glibenclamide tablet formulation in terms of BSL lowering in rabbits and diabetic human volunteers, Drug Dev. Ind. Pharm. 12 (1986) 851–866.
[14] M.T. Esclusa-Díaz, J.J. Torres-Labandeira, M. Kata, J.L. Vila-Jato, Inclusion complexation of glibenclamide with 2-hydroxypropyl-β-cyclodextrin in solution and in solid state, Eur. J. Pharm. Sci. 1 (6) (1994) 291–296.
[15] M. Valleri, P. Mura, F. Maestrelli, M. Cirri, R. Ballerini, Development and evaluation of glyburide fast dissolving tablets using solid dispersion technique, Drug Dev. Ind. Pharm. 30 (5) (2004) 525–534.
[16] B. Tashtoush, Z.S. Al-qashi, N.M. Najib, *In vitro* and *in vivo* evaluation of glibenclamide in solid dispersion systems, Drug Dev. Ind. Pharm. 30 (6) (2004) 601–607.
[17] W. Rupp, M. Badian, W. Heptner, V. Malerczyk, Bioavailability and in vitro liberation of glibenclamide from a new dosage form, Biopharm. Pharmacokinet. Eur. Congr. 2 1 (1984) 413–420.
[18] M.A. Hassan, M. Sheikh Salem, E. Sallam, M.K. Al-Hindawi, Preparation and characterization of a new polymorphic form and a solvate of glibenclamide, Acta Pharmceutica Hungarica 67 (2–3) (1997) 81–88.
[19] H.J. Arnqvist, B.E. Karlberg, A. Melander, Pharmacokinetics and effects of glibenclamide in two formulations, HB 419 and HB 420, in type 2 diabetes, Ann. Clin. Res. 15 (Suppl. 37) (1983) 21–25.
[20] P. Timmins, P.H. Marathe, G. Cave, M.E. Arnold, A.B. Dennis, D.S. Greene, Development of a glyburide-metformin fixed combination tablet with optimized glyburide particle size, Drug Dev. Ind. Pharm. 66 (2006) 25–35.
[21] H. Wei, R. Löbenberg, Biorelevant dissolution media as a predictive tool for glyburide a class II drug, Eur. J. Pharm. Sci. 29 (2006) 45–52.
[22] Personal communication with Dr. Izzy Kanfer, Faculty of Pharmacy, Rhodes University, South Africa.
[23] Guidance for Industry: Extended Release Oral Dosage Forms: Development, Evaluation and Application of *in vitro*/*in vivo* Correlations, U.S. Department of Health Food and Drug Administration Center for Drug Evaluation and Research, 1997.

[24] V. Chikhalia, R.T. Forbes, R.A. Storey, M. Ticehurst, The effect of crystal morphology and mill type on milling induced crystal disorder, Eur. J. Pharm. Sci. 27 (2006) 19–26.
[25] A. Salekigerhardt, C. Ahlneck, G. Zografi, Assessment of disorder in crystalline solids, Int. J. Pharm. 101 (3) (1994) 237–247.
[26] A. Szép, G.Y. Marosi, M. Bálint, A. Bódis, Micro-Raman spectroscopy of solid pharmaceuticals, in: Proceedings of the 8th Polymers for Advanced Technologies International Symposium, vol. 9, Budapest, Hungary, 2005, pp. 13–16.
[27] Polymer Science Learning Center, Department of Polymer Science, The University of Southern Mississippi, http://pslc.ws/macrog//dsc.htm
[28] D. Brockmeier, H.G. Grigoleit, H. Leonhardt, Absorption of glibenclamide from different sites of the gastro-intestinal tract, Eur. J. Clin. Pharmacol. 29 (2) (1985) 193–197.
[29] R.M. Atkinson, C. Bedord, K.J. Child, E.J. Tomich, Effect of particle size on blood griseofulvin levels in man, Nature 193 (1962) 588–589.
[30] M.S. Suleiman, N.M. Najib, Isolation and physicochemical characterization of solid forms of glibenclamide, Int. J. Pharm. 50 (2) (1989) 103–109.
[31] G. Balan, P. Timmins, D.S. Greene, P.H. Marathe, In-vitro In-vivo correlation models for glibenclamide after administration of metformin/glibenclamide tablets to healthy human volunteers, J. Pharm. Pharmacol. 52 (2000) 831–838.
[32] T. Rydberg, A. Jönsson, M. Karlsson, A. Meldander, Concentration-effect relations of glibenclamide and its active metabolites in man: modeling of pharmacokinetics and pharmacodynamics, Br. J. Clin. Pharmacol. 43 (1997) 373–381.